Probing halogen–halogen interactions in solution

V. Ayzac, Matthieu Raynal, B. Isare, J. Idé, P. Brocorens, R. Lazzaroni, T. Etienne, A. Monari, Xavier Assfeld, Laurent Bouteiller

Probing halogen-halogen interactions in solution

V. Ayzac,[a] M. Raynal,[a] B. Isare,[a] J. Idé,[b] P. Brocorens,[b] R. Lazzaroni,[b] T. Etienne,[c] A. Monari,[c] X. Assfeld[c] and L. Bouteiller*[a]

Halogen-halogen interactions are a particularly interesting class of halogen bonds that are known to be essential design elements in crystal engineering. In solution, it is likely that halogen-halogen interactions also play a role, but the weakness of this interaction makes it difficult to characterize or even simply detect. We have designed a supramolecular balance that allows to detect Br···Br interactions between CBr_3 groups in solution and close to room temperature. The sensitivity and versatility of the chosen platform has allowed to accumulate consistent data. In halogenoalkane solvents, we propose estimates for the free energy of these weak halogen bond interactions. In toluene solutions, we show that the interactions between Br atoms and the solvent aromatic groups dominate over the Br···Br interactions.

Introduction

Non-covalent interactions play a central role in chemistry, materials science and biology. They underlie conformational behaviour, solvation, chemical reactivity, biomolecular structure and function, crystal engineering and the bulk properties of materials. Among non-covalent interactions, halogen bonds (XB) have been the focus of much interest over the past 15 years.[1-5] The utility of XB for steering self-assembly in condensed phases has proved to be broad, encompassing applications in crystal engineering, chemical separation, topochemical polymerization and liquid crystals. Moreover, studies of XB in biomolecules have highlighted the prospect of exploiting the interaction in medicinal chemistry and drug design.[6] Alongside these applications, efforts to gain insight into the fundamental nature of the XB interactions through quantum chemical calculations have revealed the central role of electrostatic interactions that occur between the electron-rich XB acceptor and the electron-poor part (σ-hole, along the extension of the σ bond) of chlorine, bromine or iodine atoms.[7] As such, the high directionality and specificity of XB has been rationalized.

A particularly interesting class of XB interaction is the halogen-halogen (XX) interaction, which occurs in particular between two halogen atoms that are bonded to (different) carbon atoms. Although weak, these XX interactions have been shown to be essential to the formation of numerous self-assembled monolayers[8-14] and crystalline structures.[15-20] For instance, the introduction of halogen atoms at key positions allows to organize molecules in the solid state to favour topochemical polymerization,[21] or inclusion complex formation.[22] Moreover, the weak but nonetheless predictable XX interactions have been used to design crystalline solids with unusual plastic[23] or elastic[24,25] mechanical properties. Theoretical studies have allowed to rationalize the influence of the molecular structure and the electronic density distribution, on the strength of XX interactions (such as the nature of the halogen atoms, the hybridization of the carbon atoms, or substitution effects).[26,27] *In solution*, it is likely that XX interactions also play a role, but the weakness of this interaction makes it difficult to characterize or even simply detect.[28-31] As far as we know, the only demonstration of XX interactions in solution was obtained at 123K in liquid krypton (by infrared and Raman spectroscopies).[32] At room temperature, the spectral shifts associated to XX interactions are probably too small to be detected. The characterization of XX interactions in solution is therefore an open question.

A few years ago, we reported on a supramolecular balance concept that is well suited to quantify weak intermolecular effects in solution[33,34] because of its extreme sensitivity compared to similar approaches.[35,36] We now apply this concept to determine whether XX interactions can be detected and quantified in solution at room temperature.[‡]

Results and discussion

Design of the platform.

The supramolecular balance concept consists in using a solute (**1**) that self-assembles via a strong supramolecular interaction (hydrogen bonding in the present case) into two competing supramolecular assemblies. One of the assemblies is dominant at low temperature while the other prevails at high temperature. An additional weak interaction (XX interaction in the present case) that is ideally formed only in one of the assemblies acts as a perturbation that may be detected (and quantified) by measuring the transition temperature (T_1) between the two assemblies, as well as the enthalpy of the transition (Δh_1) by calorimetry.[33] Quantification requires a suitable reference compound (**0**) that assembles in the same competing structures as (**1**) but that does not form the additional weak interaction. The free energy associated to the weak interaction is then simply related to the enthalpy Δh_1 and

[a] *Sorbonne Universités, UPMC Univ Paris 06, CNRS, Institut Parisien de Chimie Moléculaire, Equipe Chimie des Polymères, 4 Place Jussieu, F-75005 Paris, France.*
[b] *Service de Chimie des Matériaux Nouveaux, Université de Mons, Place du Parc, 20, B-7000 Mons, Belgium.*
[c] *Université de Lorraine & CNRS, SRSMC, TMS, Boulevard des Aiguillettes, 54506 Vandoeuvre-lès-Nancy, France.*

Electronic Supplementary Information (ESI) available: Synthesis and characterization of bisureas. Additional SANS, FTIR, DSC, CD and molecular simulation data. See DOI: 10.1039/x0xx00000x

to the difference between the transition temperatures (T_1 and T_0) through: [‡‡]

$$\Delta\Delta G = \Delta G_1(T_0) - \Delta G_0(T_0) = \Delta h_1 \frac{T_1 - T_0}{T_0} \quad (1)$$

Based on our previous experience of the bisurea platform,[37] we designed potential candidates featuring (i) a central self-assembling bisurea core, (ii) an amino-ester connection to allow a straightforward functionalization, (iii) an alkylene flexible spacer, and (iv) a terminal CBr_3 (or CCl_3) moiety to introduce XX interactions (Fig. 1). The reference molecules with a terminal CH_3 moiety was also prepared to serve as a non-halogen bonded blank.

The targeted bisureas were synthesized with a high enantiomeric purity and characterized by NMR, HRMS and chiral HPLC (see ESI). Then, their solubility was tested to determine which solvents are suitable for further investigation (Table S1). Toluene (but also propylbenzene, 1-bromohexane and 1-chlorohexane) proved to be adequate, because they allowed to obtain homogeneous and viscoelastic solutions that are characteristic for the presence of long supramolecular assemblies at room temperature.

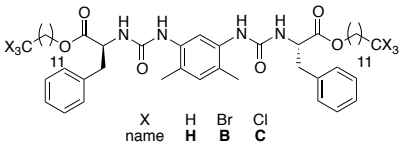

Fig. 1 Structure of bisureas.

Differential scanning calorimetry (DSC) data show an endothermal transition in the temperature range 30-80°C (Fig. 2), which means that the self-assembled bisurea structure that is stable at room temperature transforms into a less organized assembly at high temperature. SANS data (Fig. S1) show that the bisureas form long and rigid supramolecular assemblies and that the high-temperature structure differs from the low-temperature structure mainly by a twice lower linear density (Table S2). In fact, the linear densities measured by SANS are very close to those measured previously for similar bisureas.[38] The low- (high-) temperature assembly can therefore be assigned to a rod-like structure with two bisureas (one bisurea) in the cross-section. They will be called double filament and single filament, respectively. FTIR data (Fig. S2) show that the assemblies are long because the free N-H vibration band is not detected up to 70°C, i.e., 20°C above the transition temperatures.

At this point we can conclude that bisurea **B** seems to be suitable for the supramolecular balance because the endothermal peak detected in toluene corresponds to a transition between two supramolecular polymers. Moreover, bisurea **B** and its reference **H** have the same supramolecular structures, as shown by SANS, FTIR and CD analyses (Figs. S1 to S5). Finally, bisurea **B** and its reference **H** have measurably different transition temperatures, as shown by DSC or by the shape of the VT-FTIR spectra[38] (Fig. 2). However, the interpretation for this measured difference first requires a better insight in the structure of the single and double filament supramolecular assemblies.

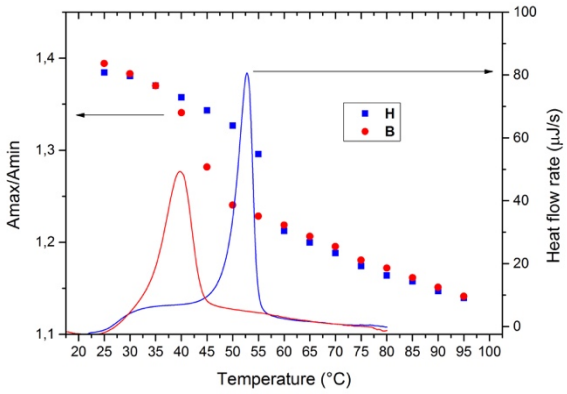

Fig. 2 DSC thermogram and FTIR absorbance ratio (measured at 3325cm^{-1} (max) and 3295cm^{-1} (min)) for solutions of bisurea **B** (red data) or **H** (blue data) in toluene (10 mM, heating run, 1°C/min).

Molecular simulations.

Molecular models of the assemblies are needed to check whether Br···Br interactions can be involved in one or in both supramolecular assemblies. First, a set of possible structures was constructed and evaluated in vacuum for a model bisurea monomer having a CH_3 side group instead of a long alkyl chain in **B** and **H**. These structures differ by the number of bisurea molecules in the cross-section and the molecular arrangement of the bisurea molecules (see ESI). Among these, a single helix and a double helix (shown in Fig. 3) were found to be the most stable structures and provided geometrical features in agreement with SANS data. It must be noted that the helical arrangement of the bisurea molecules in these structures is in accordance with the CD analyses, which reveal that both the low- and high-temperature structures are chiral at the supramolecular level (Fig. S5). It is therefore hypothesized that these two structures represent reasonably well the actual hydrogen-bond network and molecular arrangement present in the low- and high-temperature assemblies.

We next constructed the single helix and double helix structures of **B** in chlorohexane and found out that neither the introduction of long brominated alkyl chains nor the presence of the solvent change significantly the structural parameters of the core of the filaments. The calculated CD spectra and the linear densities are also in qualitative agreement with those measured experimentally (see ESI). Hence, both experimental data (SANS, CD, IR) and theoretical data indicate that bisurea **B** and **H** have similar structures for the core of the filaments, which are thus not influenced by the nature of the end-groups. This result is not surprising, as the chemical modifications are made at the very end of the side chains, far from the core of the molecules where the interactions driving the assembly take place.

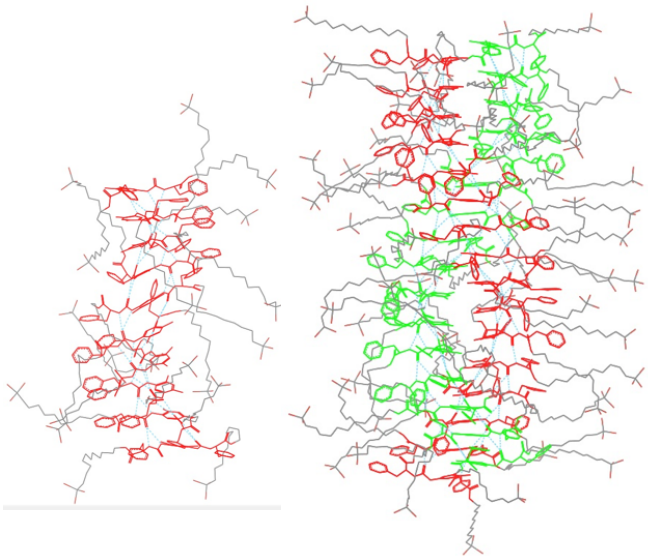

Fig. 3 Proposed structure for the single (left) and double filament (right) assemblies formed by bisurea **B**. The structures were obtained by MD simulations (20ns) in an explicit solvent box (1-chlorohexane). The core of the molecules is highlighted in colour and the hydrogen atoms were removed for the sake of clarity. The number of monomers displayed corresponds to a complete helix turn.

Fig. 4 shows the radial distribution functions calculated between CBr_3 end groups for the simulated assemblies of **B**. The first peak at 6.1Å corresponds to direct contacts between CBr_3 groups. The cumulative number of CBr_3 groups located at a given distance from a given CBr_3 group have been extracted from these distributions. The data show that there are about three times more contacts between CBr_3 groups in the double filament than in the single filament: about 1.53 and 0.53 contacts per CBr_3 group, respectively, when integrating the first peak up to the minimum at 8.8Å. Similar results are obtained if the distance between Br atoms is monitored (see Fig. S15). This result is consistent with the denser packing in the double helix structure. It also implies that the value of the transition temperature should be directly influenced by the strength of XX interactions, thus confirming the validity of this bisurea platform as a supramolecular balance. More precisely, these results mean that the double helix structure for **B** should be stabilized by the larger number of Br···Br contacts. Therefore, if solvation effects are negligible, then the transition temperature for **B** should be above the transition temperature for **H**.

In fact, the experimental results in toluene (Fig. 2) show the opposite effect: the transition temperature is lower for the brominated system, which means that the double filament structure is less stabilized (with respect to the single filament) when CH_3 groups are replaced by CBr_3 groups. This could be due to a significant effect of solvation,[39] if CBr_3···solvent contacts are more favourable than CH_3···solvent contacts. Such an effect should stabilize the single filament structure of **B** because its less dense packing (compared to the double filament) allows more contacts with the solvent. In order to discriminate solvation effects from Br···Br interactions, we tested two complementary approaches.

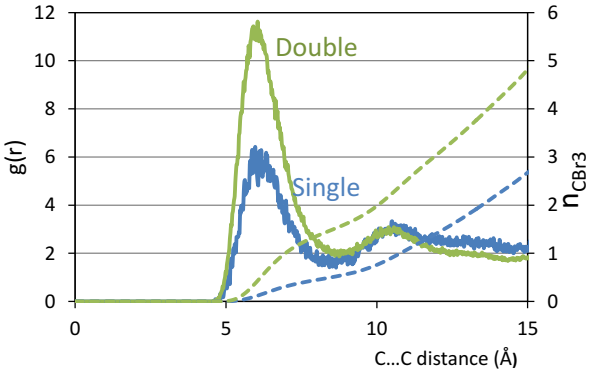

Fig. 4 Intermolecular radial distribution function, g(r), between CBr_3 end groups (continuous lines), and cumulative number of neighbouring CBr_3 (dashed lines) as a function of the C···C distance between CBr_3 groups, for the single (blue lines) or double (green lines) filaments.

Analysis of the data in series of similar solvents.

Our first approach is to test whether the difference between the transition temperatures measured for **B** and **H** ($\Delta T = T_B - T_H$) depends on the solvent. Three families of solvents were considered: alkylbenzenes (Fig. 5), chloroalkanes and bromoalkanes (Fig. 6). The absolute variation of the transition temperatures (T_B and T_H) is dominated by the effect of the solvent on the main interactions in the system (i.e., involving the core of the molecules). By examining the ΔT values instead, we cancel out the effect of those main interactions and allow focusing on the differences brought by the CBr_3 and CH_3 moieties. In the case of alkylbenzene solvents, the fact that ΔT strongly depends on the solvent is a direct indication that solvation effects play an important role on the interactions involving the CX_3 moieties. Moreover, the sign of ΔT changes from positive to negative from pentylbenzene to toluene, which means that the single filament of **B** is more stabilized by toluene than by pentylbenzene (when compared to the filament of **H**). Since the single filament structure is more accessible to the solvent than the double filament and since the concentration of aromatic groups is larger in toluene than in pentylbenzene, the data indicate that CBr_3···aromatic interactions are more favourable than CH_3···aromatic interactions (and/or CBr_3···methylene interactions are less favourable than CH_3···methylene interactions). In any case, if XX interactions are to be probed, less competing solvents are required.

In chloroalkanes, we also observe a quasi-linear evolution of the transition temperature with the size of the alkyl chain. However, ΔT is positive and independent of the solvent for both **B** and **C**, thus showing a constant influence of the solvent (Fig. 6). In bromoalkanes, the same situation is observed except that ΔT is smaller and close to zero in the case of **C**. These results show that for these systems, solvation effects are negligible compared to the interactions among CBr_3, CCl_3, and CH_3 groups, or at least that these solvation effects are constant, i.e., not affected by the relative proportion of halogen and

methylene groups in the solvent. Qualitatively, these results also show that CBr_3 groups affect the stability of the assemblies more than CCl_3 groups, which is in line with an expected Br···Br interaction stronger than Cl···Cl. Moreover, the effect is less intense in bromoalkanes, which are expected to compete more than chloroalkanes for the formation of halogen bonds. It may seem surprising that bromo- and chloroalkane solvents appear to interfere less with intermolecular CBr_3 interactions than aromatic solvents, but it is known that aromatic π-systems are better halogen bond acceptors than halogens themselves.[40]

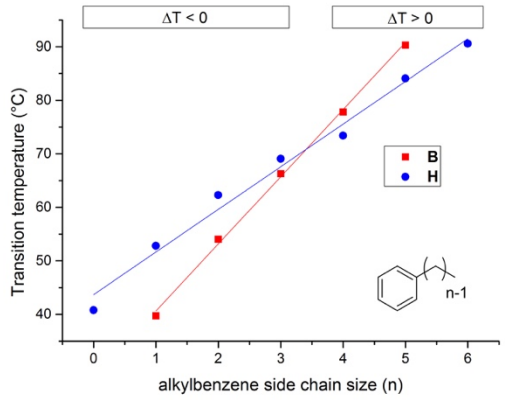

Fig. 5 Transition temperature for solutions of bisurea **B** or **H** in alkylbenzenes ($C_nH_{2n+1}C_6H_5$) versus the size of the solvent alkyl chain (n) (10 mM measured by nDSC). The lines are drawn as a guide to the eye.

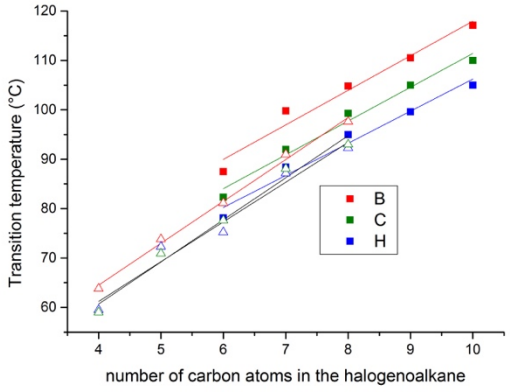

Fig. 6 Transition temperature for solutions of bisurea **B**, **C** or **H** in 1-chloroalkanes ($C_nH_{2n+1}Cl$) (squares) or in 1-bromoalkanes ($C_nH_{2n+1}Br$) (triangles) versus the size of the solvent alkyl chain (n) (10 mM measured by nDSC). The lines are drawn as a guide to the eye.

Analysis of the data for mixtures of bisureas.

To further discriminate solvation effects from Br···Br interactions, our second approach is to mix brominated (**B**) and non-brominated (**H**) bisureas in various ratios and to measure the transition temperatures in a given solvent (Fig. 7). We expect mixtures of bisureas to form statistical co-assemblies[41] and we postulate that if the change in the transition temperature is mainly due to solvation or steric effects, we should observe a linear evolution of the transition temperature with the composition. In contrast, if the interactions between **B** molecules within the assembly are dominant, we should observe a quadratic evolution. To confirm this intuitive idea and to be able to extract quantitative data from Fig. 7, we propose a simple model.

We call S_x (D_x) the single (double) filament composed of a mixture of x **B** and 1-x **H** bisureas. At the transition temperature T_x, if we assume that a double filament dissociates into two single filaments, the free energy change of the system is:

$$\Delta G(x) = 2\,G(S_x) - G(D_x) \quad (2)$$

where we normalize the free energy by the number of CBr_3 and CH_3 groups, i.e., by twice the number of bisurea molecules. By doing so, we neglect chain-end effects of the supramolecular assemblies. We then decompose the free energy of the single filament as:

$$G(S_x) = G_{core}(S) + G_{end}(S_x) + G_{solv\ core}(S) + G_{solv\ end}(S_x) \quad (3)$$

where $G_{core}(S)$ corresponds to the main interactions between bisureas that stabilize the single filament. These (mainly hydrogen bond) interactions between the core of the molecules are expected to be independent of *x*. $G_{end}(S_x)$ takes into account the interactions between the end of the molecules (CH_3 and CBr_3 groups) and $G_{solv\ core}(S)$ ($G_{solv\ end}(S_x)$) corresponds to the interactions between the solvent and the core of the molecules (the end of the molecules) in the single filament. Similarly, we decompose the free energy of the double filament as:

$$G(D_x) = G_{core}(D) + G_{end}(D_x) + G_{solv\ core}(D) + G_{solv\ core}(D_x) \quad (4)$$

Replacing equations (3) and (4) into equation (2) yields:

$$\Delta G(x) = \Delta G_{core} + \Delta G_{end}(x) + \Delta G_{solv\ core} + \Delta G_{solv\ end}(x) \quad (5)$$

where we define ΔG_{core}, the variation of the interactions between the bisurea cores when a double filament is converted into two single filaments, as:

$$\Delta G_{core} = 2\,G_{core}(S) - G_{core}(D) \quad (6)$$

$\Delta G_{end}(x)$ is the variation of interactions between CX_3 groups when a double filament is converted into two single filaments:

$$\Delta G_{end}(x) = 2\,G_{end}(S_x) - G_{end}(D_x) \quad (7)$$

$\Delta G_{solv\ core}$ is the variation of solvation of the core of the molecules when a double filament is converted into two single filaments:

$$\Delta G_{solv\ core} = 2\,G_{solv\ core}(S) - G_{solv\ core}(D) \quad (8)$$

and $\Delta G_{solv\ end}(x)$ is the variation of solvation of the end of the molecules when a double filament is converted into two single filaments:

$$\Delta G_{solv\ end}(x) = 2\,G_{solv\ end}(S_x) - G_{solv\ end}(D_x) \quad (9)$$

Now, if we take the composition x=0 as the reference (pure **H**):

$$\Delta\Delta G(x) = \Delta G(x) - \Delta G(0) = \Delta\Delta G_{end}(x) + \Delta\Delta G_{solv}(x) \quad (10)$$

with

$$\Delta\Delta G_{end}(x) = \Delta G_{end}(x) - \Delta G_{end}(0) \quad (11)$$

and

$$\Delta\Delta G_{solv}(x) = \Delta G_{solv\ end}(x) - \Delta G_{solv\ end}(0) \quad (12)$$

We now define G_{BB} as the free energy of interaction between two CBr_3 groups (i.e., a XX interaction);[§] G_{BH} as the free energy of interaction between a CBr_3 group and a CH_3 group (i.e., mainly a weak electrostatic interaction); and G_{HH} as the free energy of interaction between two CH_3 groups (i.e., a London interaction).[§§] The number of contacts per end groups that are

lost at the transition is named λ. Because of the low values of the free energy of the interactions considered, λ is supposed to be independent of *x*, i.e., dominated by entropy. Finally, if we assume a statistical distribution of the CBr_3 and CH_3 groups in the assemblies:

$\Delta G_{end}(x) = -\lambda [x^2 G_{BB} + 2x(1-x) G_{BH} + (1-x)^2 G_{HH}]$ (13)

and

$\Delta\Delta G_{end}(x) = -\lambda x^2 [G_{BB} - 2 G_{BH} + G_{HH}] - 2\lambda x [G_{BH} - G_{HH}]$ (14)

In contrast, since solvation depends on the contact between each monomer and the solvent, it can be expected to be a linear function of the composition:

$G_{solv\ end}(S_x) = x\ G_{solv\ end}(S_1) + (1-x)\ G_{solv\ end}(S_0)$ (15)

and

$G_{solv\ end}(D_x) = x\ G_{solv\ end}(D_1) + (1-x)\ G_{solv\ end}(D_0)$ (16)

Therefore, replacing (15) and (16) into (9) and (12) yields:

$\Delta\Delta G_{solv}(x) = x\ (\Delta G_{solv\ end}(1) - \Delta G_{solv\ end}(0))$ (17)

Since the variation of solvation only concerns the number of contacts between end groups that are actually lost at the transition (λ), then:

$\Delta\Delta G_{solv}(x) = \lambda x\ (\Delta G_{solv}(CBr_3) - \Delta G_{solv}(CH_3))$ (18)

where $\Delta G_{solv}(CBr_3)$ ($\Delta G_{solv}(CH_3)$) is the variation of solvation of a CBr_3 group (of a CH_3 group) when a double filament is converted into two single filaments.

Combining equations (14) and (18) into (10) yields

$\Delta\Delta G(x) = \lambda x [\Delta G_{solv}(CBr_3) - \Delta G_{solv}(CH_3) - 2 G_{BH} + 2 G_{HH}] - \lambda x^2 [G_{BB} - 2 G_{BH} + G_{HH}]$ (19)

Equivalently, instead of considering the bare interactions G_{XY}, we can consider the same interactions in the solvent (i.e., which include partial desolvation): G_{XY}^{solv}.

$G_{BB}^{solv} = G_{BB} - \Delta G_{solv}(CBr_3)$ (20)

$G_{BH}^{solv} = G_{BH} - \frac{1}{2}\Delta G_{solv}(CBr_3) - \frac{1}{2}\Delta G_{solv}(CH_3)$ (21)

$G_{HH}^{solv} = G_{HH} - \Delta G_{solv}(CH_3)$ (22)

$\Delta\Delta G(x) = 2\lambda x\left(G_{HH}^{solv} - G_{BH}^{solv}\right) - \lambda x^2(G_{BB}^{solv} - 2G_{BH}^{solv} + G_{HH}^{solv})$ (23)

If we neglect London interactions compared to electrostatic interactions and halogen-halogen interactions, then:

$\Delta\Delta G(x) \approx \lambda x\ (\Delta\Delta G_{solv} - 2\ G_{BH}) - \lambda x^2\ (G_{BB} - 2\ G_{BH})$ (24)

where $\Delta\Delta G_{solv} = \Delta G_{solv}(CBr_3) - \Delta G_{solv}(CH_3)$, or equivalently

$\Delta\Delta G(x) \approx -2\lambda x G_{BH}^{solv} - \lambda x^2(G_{BB}^{solv} - 2G_{BH}^{solv})$ (25)

Finally, if we combine equations (1) and (24) or (25), we obtain an expression for the transition temperature of a mixture containing x **B** and 1-x **H** bisureas:

$T(x) \approx T(0)\left[1 + \frac{\lambda x(\Delta\Delta G_{solv} - 2G_{BH}) - \lambda x^2(G_{BB} - 2G_{BH})}{\Delta h_1}\right]$ (26)

or equivalently

$T(x) \approx T(0)\left[1 - \frac{2\lambda x G_{BH}^{solv} + \lambda x^2(G_{BB}^{solv} - 2G_{BH}^{solv})}{\Delta h_1}\right]$ (27)

Equations (26) or (27) can be used to analyse the data of Fig. 7. In the case of mixtures in toluene, the enthalpy measured by calorimetry is Δh_1 = 5.7 kJ/mol and the fit with equation (26) yields $\lambda(\Delta\Delta G_{solv} - 2\ G_{BH}) = -220$ J/mol and $\lambda|G_{BB} - 2\ G_{BH}| << 220$ J/mol, i.e. the quadratic term is negligible. As in the case of the first approach (Fig. 5), this result can be interpreted by the dominance of solvation, i.e., CBr_3···aromatic interactions stabilize the single filament structure more than CBr_3···CBr_3 interactions stabilize the double filament structure.

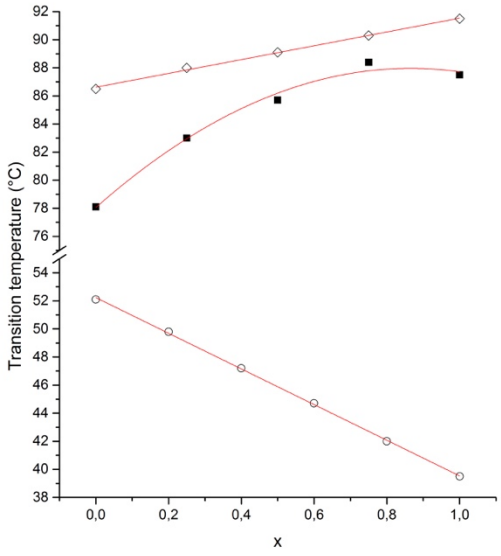

Fig. 7 Transition temperature for mixtures of bisureas **B** and **H** in toluene (hollow circles), 1-chlorohexane (full squares) or 1-bromoheptane (hollow diamonds) (10 mM measured by nDSC). x=0 is pure **H**; x=1 is pure **B**; the full lines represent the best fits with equations (26) or (27).

In chlorohexane, both mixtures **H**/**B** (Fig. 7) and **H**/**C** (Fig. S7) display a non-linear variation of the transition temperature versus the composition. For **B**, the measured enthalpy is Δh_1 = 4.3 kJ/mol and the fit of the data with equation (27) yields values for $\lambda G_{BH}^{Clhexane} = -140\ J/mol$ and $\lambda G_{BB}^{Clhexane} = -120\ J/mol$. In order to deduce the actual interaction energies we need to estimate the fraction of contacts affected by the double filament/single filament transition (λ). This correction factor can be estimated from the simulation data of Fig. 4. We can consider that the first peak of the radial distribution function represents the fraction of interacting CBr_3 groups. It means that we can apply a cut-off value of 8.8Å to estimate the number of interacting CBr_3 groups from the value of the cumulative number of neighbouring CBr_3 groups. The difference between this value for the double filament structure (1.53) and for the single filament structure (0.53) provides an estimate for the number of CBr_3 neighbours lost at the double filament/single filament transition, i.e. $\lambda \approx 1.53 - 0.53 \approx 1$. In Table S3, the values have therefore been corrected by this factor. The same approach was applied to the data of **H**/**C** mixtures in chlorohexane (Fig. S7) and of **H**/**B** mixtures in bromoheptane (Fig. 7). The results are summarized in Table S3. Several comments can be made. First, in solution, the XX interactions between CX_3 groups (G_{XX}^{solv}) are of the same order of magnitude as the corresponding interactions between CX_3 and CH_3 groups (G_{XH}^{solv}). Second, both kinds of interactions are weaker in bromoheptane than in chlorohexane. Finally, the Cl···Cl interactions are significantly weaker than the Br···Br interactions, as expected.

Coming back to the data of Fig. 6, it is possible to analyse the shifts between the plots in the light of our simple thermodynamic model. Indeed, for x = 1, equation (27) simplifies to

$$\lambda G_{BB}^{solv} \approx -\Delta h_1 \left(\frac{T(1)-T(0)}{T(0)}\right) \quad (28)$$

The data of Fig. 6 were then plotted according to this expression: Fig. 8 shows that in chloroalkanes, $G_{BB}^{Clalkane}$ and $G_{CC}^{Clalkane}$ are independent of the solvent and the average values deduced from the plots (Table S4) are very similar to the values in Table S3. Therefore, both approaches (altering solvent or mixing bisureas) are consistent. This is not completely surprising as the experimental value for x = 1 in chlorohexane is common to both data sets, but it is nevertheless an indication of the coherence of the approaches. In bromoalkanes, the data are also in qualitative agreement with Table S3, but the weaker interactions involved preclude a more quantitative analysis.

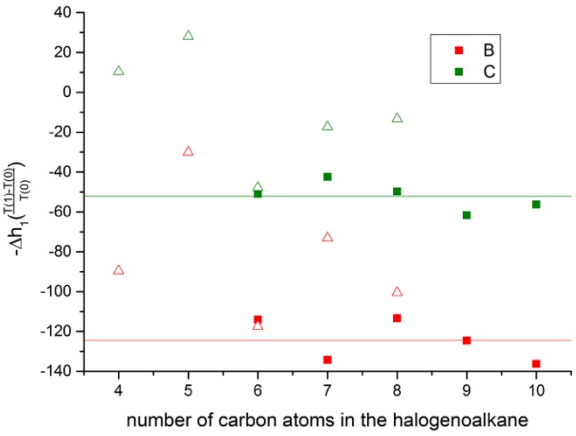

Fig. 8 Evolution of $-\Delta h_1 \left(\frac{T(1)-T(0)}{T(0)}\right)$ for solutions of bisurea **B** or **C** in 1-chloroalkanes ($C_nH_{2n+1}Cl$) (squares) or in 1-bromoalkanes ($C_nH_{2n+1}Br$) (triangles) versus the size of the solvent alkyl chain (n) (same data as in Fig. 6).

Conclusions

The precise quantification and rationalization of the interaction free energy of several classes of XB interactions constitute a challenge for conventional methods due to the weak nature of these interactions. In the solid state, the rigid nature of the assemblies makes the detection and quantification of XB possible, and to a certain extent straightforward. In contrast, in liquid or soft-matter systems the increased flexibility and mobility of the constituents, coupled with the crucial solvation interactions necessitate tailored approaches. Here, we report the suitability of a supramolecular balance approach to tackle this problem.

The approach consists in measuring the transition temperature between double helix and single helix supramolecular structures by calorimetry, with the double helix being more stabilized by XX interactions than the single helix. The last point was clearly established by MM/MD calculations showing that approximately a full CX_3-CX_3 contact is lost per CX_3 group during the structural transition between the double helix and the single helix structures.

We show that this approach allows detecting, to the best of our knowledge for the first time, Br···Br, Cl···Cl, Br···H and Cl···H interactions between CBr_3, CCl_3 and CH_3 groups in solution and around room temperature. Furthermore, the sensitivity and versatility of the chosen platform has allowed to accumulate a set of highly consistent data, allowing not only a qualitative observation of XX interactions and their role in guiding supramolecular aggregation, but also to quantitatively estimate their strengths in terms of free energy. The role of the solvent has been proved to be fundamental in this context. In particular, in halogenated alkane solvents, we propose estimates for the free energy of these weak halogen bond and weak electrostatic interactions. On the contrary, in toluene solutions, we show that the interactions between Br atoms and the solvent aromatic groups dominate over the Br···Br interactions.

We are aware that our model should be further tested. In particular, the limited control over the orientation of the interacting CX_3 groups entails a significant uncertainty over the energetic values proposed. It should be possible to confirm the reliability of these estimates by comparison with related data, i.e., by checking the independence of the results from the actual choice of the platform. In addition, from a molecular modelling point of view, it could be possible to directly access the solvation and interaction free energy values for controlled systems, thanks to the adequate sampling of the conformational space offered for instance by alchemical transformations and free energy perturbation.[42]

Conflicts of interest

There are no conflicts to declare.

Acknowledgements

This work was supported by the French Agence Nationale de la Recherche (project ANR-12-BS08-0019 BalanceSupra). Jacques Jestin (LLB, Saclay) is acknowledged for assistance with the SANS experiments, and Nicolas Vanthuyne (iSm2, Marseille) for chiral HPLC analyses. Research in Mons is also supported by the Belgian Federal Government (BELSPO PAI VII-5 program) and FNRS (CECI program).

Notes and references

‡ Various halogen bonds have been successfully characterized in solution with similar approaches,[43-46] but not XX interactions which are particularly weak halogen bonds involving C-X as both acceptor and donor.

‡‡ In this approach, we assume cross-interactions between the strongly and weakly interacting groups to be negligible.

§ The free energy is normalized by the number of CBr_3 groups, so that it actually corresponds to half of a XX interaction.

§§ Analogously, we define G_{CC} as the free energy of interaction between two CCl_3 groups and G_{CH} as the free energy of interaction between a CCl_3 group and a CH_3 group.

1 P. Metrangolo, F. Meyer, T. Pilati, G. Resnati and G. Terraneo, *Angew. Chem. Int. Ed.*, 2008, **47**, 6114–6127.

2 P. Politzer, J. S. Murray and T. Clark, *Phys. Chem. Chem. Phys.*, 2013, **15**, 11178–11189.

3 A. Mukherjee, S. Tothadi and G. R. Desiraju, *Acc. Chem. Res.*, 2014, **47**, 2514–2524.

4 G. Cavallo, P. Metrangolo, R. Milani, T. Pilati, A. Priimagi, G. Resnati and G. Terraneo, *Chem. Rev.*, 2016, **116**, 2478–601.

5 C. C. Robertson, J. S. Wright, E. J. Carrington, R. N. Perutz, C. A. Hunter and L. Brammer, *Chem. Sci.*, 2017, **8**, 5392–5398.

6 H. Matter, M. Nazare, S. Guessregen, D. W. Will, H. Schreuder, A. Bauer, M. Urmann, K. Ritter, M. Wagner and V. Wehner, *Angew. Chem. Int. Ed.*, 2009, **48**, 2911–2916.

7 T. Clark, M. Hennemann, J. S. Murray and P. Politzer, *J. Mol. Model.*, 2007, **13**, 291–296.

8 H. Walch, R. Gutzler, T. Sirtl, G. Eder and M. Lackinger, *J. Phys. Chem. C*, 2010, **114**, 12604–12609.

9 J. K. Yoon, W. Son, K.-H. Chung, H. Kim, S. Han and S.-J. Kahng, *J. Phys. Chem. C*, 2011, **115**, 2297–2301.

10 R. Gutzler, O. Ivasenko, C. Fu, J. L. Brusso, F. Rosei and D. F. Perepichka, *Chem. Commun.*, 2011, **47**, 9453–9455.

11 W. Song, N. Martsinovich, W. M. Heckl and M. Lackinger, *Chem. Commun.*, 2014, **50**, 13465–13468.

12 X. Hu, B. Zha, Y. Wu, X. Miao and W. Deng, *Phys. Chem. Chem. Phys.*, 2016, **18**, 7208–7215.

13 Y. Wu, J. Li, Y. Yuan, M. Dong, B. Zha, X. Miao, Y. Hu and W. Deng, *Phys. Chem. Chem. Phys.*, 2017, **19**, 3143–3150.

14 B. Zha, M. Dong, X. Miao, S. Peng, Y. Wu, K. Miao, Y. Hu and W. Deng, *Nanoscale*, 2017, **9**, 237–250.

15 G. R. Desiraju and R. Parthasarathy, *J. Am. Chem. Soc.*, 1989, **111**, 8725–6.

16 V. R. Pedireddi, D. S. Reddy, B. S. Goud, D. C. Craig, A. D. Rae and G. R. Desiraju, *J. Chem. Soc. Perkin Trans. 2 Phys. Org. Chem.*, 1994, 2353–60.

17 S. Samai and K. Biradha, *CrystEngComm*, 2009, **11**, 482–492.

18 S. F. Haddad, R. D. Willett and B. Twamley, *J. Chem. Crystallogr.*, 2010, **40**, 902–908.

19 S. Tothadi, S. Joseph and G. R. Desiraju, *Cryst. Growth Des.*, 2013, **13**, 3242–3254.

20 Y. Sonoda, M. Goto, Y. Matsumoto, Y. Shimoi, F. Sasaki and A. Furube, *Cryst. Growth Des.*, 2016, **16**, 4060–4071.

21 A. Matsumoto, T. Tanaka, T. Tsubouchi, K. Tashiro, S. Saragai and S. Nakamoto, *J. Am. Chem. Soc.*, 2002, **124**, 8891–8902.

22 K. Tanaka, D. Fujimoto and F. Toda, *Tetrahedron Lett.*, 2000, **41**, 6095–6099.

23 C. M. Reddy, M. T. Kirchner, R. C. Gundakaram, K. A. Padmanabhan and G. R. Desiraju, *Chem. - Eur. J.*, 2006, **12**, 2222–2234.

24 S. Ghosh, M. K. Mishra, S. B. Kadambi, U. Ramamurty and G. R. Desiraju, *Angew. Chem. Int. Ed.*, 2015, **54**, 2674–2678.

25 S. Saha and G. R. Desiraju, *Chem. – Eur. J.*, 2017, **23**, 4936–4943.

26 F. F. Awwadi, R. D. Willett, K. A. Peterson and B. Twamley, *Chem. - Eur. J.*, 2006, **12**, 8952–8960.

27 T. T. T. Bui, S. Dahaoui, C. Lecomte, G. R. Desiraju and E. Espinosa, *Angew. Chem. Int. Ed.*, 2009, **48**, 3838–3841.

28 M. Erdelyi, *Chem. Soc. Rev.*, 2012, **41**, 3547–3557.

29 T. M. Beale, M. G. Chudzinski, M. G. Sarwar and M. S. Taylor, *Chem. Soc. Rev.*, 2013, **42**, 1667–1680.

30 A.-C. C. Carlsson, A. X. Veiga and M. Erdelyi, *Top. Curr. Chem.*, 2015, **359**, 49–76.

31 A. V. Jentzsch, *Pure Appl. Chem.*, 2015, **87**, 15–41.

32 D. Hauchecorne and W. A. Herrebout, *J. Phys. Chem. A*, 2013, **117**, 11548–11557.

33 M. Roman, C. Cannizzo, T. Pinault, B. Isare, B. Andrioletti, P. van der Schoot and L. Bouteiller, *J. Am. Chem. Soc.*, 2010, **132**, 16818–16824.

34 L. Bouteiller and P. van der Schoot, *J. Am. Chem. Soc.*, 2012, **134**, 1363–1366.

35 I. K. Mati and S. L. Cockroft, *Chem. Soc. Rev.*, 2010, **39**, 4195–4205.

36 S. L. Cockroft and C. A. Hunter, *Chem. Soc. Rev.*, 2007, **36**, 172–188.

37 B. Isare, S. Pensec, M. Raynal and L. Bouteiller, *Comptes Rendus Chim.*, 2016, **19**, 148–156.

38 M. Dirany, V. Ayzac, B. Isare, M. Raynal and L. Bouteiller, *Langmuir*, 2015, **31**, 11443–11451.

39 S. L. Cockroft and C. A. Hunter, *Chem. Commun.*, 2006, 3806–3808.

40 J. A. Webb, J. E. Klijn, P. A. Hill, J. L. Bennett and N. S. Goroff, *J. Org. Chem.*, 2004, **69**, 660–664.

41 B. Isare, L. Bouteiller, G. Ducouret and F. Lequeux, *Supramol. Chem.*, 2009, **21**, 416–421.

42 M. Aldeghi, A. Heifetz, M. J. Bodkin, S. Knapp and P. C. Biggin, *Chem. Sci.*, 2016, **7**, 207–218.

43 A. R. Voth, F. A. Hays and P. S. Ho, *Proc. Natl. Acad. Sci.*, 2007, **104**, 6188–6193.

44 E. Danelius, H. Andersson, P. Jarvoll, K. Lood, J. Gräfenstein and M. Erdélyi, *Biochemistry*, 2017, **56**, 3265–3272.

45 M. R. Scholfield, M. C. Ford, A.-C. C. Carlsson, H. Butta, R. A. Mehl and P. S. Ho, *Biochemistry*, 2017, **56**, 2794–2802.

46 H. Sun, A. Horatscheck, V. Martos, M. Bartetzko, U. Uhrig, D. Lentz, P. Schmieder and M. Nazaré, *Angew. Chem. Int. Ed.*, 2017, **56**, 6454–6458.